

# ON THE EFFECT OF FRAUNHOFER LINES ON $U$ , $B$ , $V$ MEASUREMENTS

R. L. WILDEY, E. M. BURBIDGE,\* A. R. SANDAGE, AND G. R. BURBIDGE\*

Mount Wilson and Palomar Observatories

Carnegie Institution of Washington, California Institute of Technology

*Received May 22, 1961; revised August 24, 1961*

## ABSTRACT

The effect on the observed  $U$ ,  $B$ , and  $V$  magnitudes of the removal of the Fraunhofer lines from the spectra of  $\xi$  Peg (F7 V), 50 And (F8 V), the center of the solar disk (G0 V), and HD 19445 (sdF) is assessed by the measurement on direct-intensity microphotometer tracings of the energy abstracted from the continuum by the absorption lines. The star 70 Vir (G5 V) has also been measured in part, but it was impossible to place the continuum in the ultraviolet region by empirical means because of the extreme crowding of the lines. The effect on the colors caused by (1) blocking of the radiation by the Fraunhofer lines and (2) the back-warming effect due to radiation back-scattered into the photosphere is considered. The slopes of the blanketing vectors in the  $U - B$ ,  $B - V$  diagram are determined as a function of their  $B - V$  intersection with the Hyades relation. From the slopes, a family of curves has been constructed which allow corrections  $\Delta(B - V)$ ,  $\Delta(U - B)$ , and  $\Delta V$  to be applied to any weak-lined star to reduce the  $U$ ,  $B$ , and  $V$  observations to those for stars with as strong metal lines as the Hyades stars. These corrections, given in Table 4, are a function of the observed  $B - V$  and the observed ultraviolet excess  $\delta(U - B)$  alone. Previous conclusions that most mild subdwarfs are explicable in terms of line blanketing are preserved.

## I. INTRODUCTION

With Miss Roman's discovery (1954) of a large ultraviolet excess in the radiation of subdwarf stars and with the subsequent identification of stars on the main sequences of globular clusters with subdwarfs (by many authors), a serious technical problem has arisen in obtaining photometric parallaxes. The zero-age main sequence normally used for fitting the main sequences of clusters and hence obtaining  $\pi_{pt}$  is defined at the faint end by stars in the Hyades cluster. These stars, when plotted in a two-color diagram, lie on the usual relation between  $U - B$  and  $B - V$  which is defined by solar-neighborhood stars with normal metal abundance. However, the stars of low metal content, such as the subdwarfs, cannot be analyzed with these color-magnitude and color-color diagrams until corrections have been made for the effect of the weakness of the Fraunhofer lines on the  $U$ ,  $B$ ,  $V$  measurements.

Strömberg (unpublished) was apparently the first to suggest that the ultraviolet excess found in subdwarfs might be due to the weakness of the Fraunhofer lines in their spectra. The absorption lines due to the metals are stronger and are crowded more closely in the blue spectral region than in the visual and still more in the ultraviolet than in the blue. Consequently, through the blanketing effect of the spectral lines, the radiation leaving a star like the sun is diminished progressively toward shorter wavelengths as compared with the radiation leaving a hypothetical star of equivalent effective temperature with no spectral lines. The effect is clearly less for a star with low metal content than it is for a star with solar abundances; the surface layers of such a star would let through more blue radiation relative to the visual and still more ultraviolet relative to the blue than would be the case in the sun. Such an effect could qualitatively explain the ultraviolet excess in the radiation of stars of low metal content and also the existence of a subdwarf sequence in the color-magnitude diagram, since a shift to the left off the main sequence is equivalent to causing a star to lie below the main sequence.

A test of Strömberg's suggestion was made by Schwarzschild, Searle, and Howard

\* Now at the University of Chicago.

(1955) by spectrophotometry of the blue and visual spectral regions of two normal dwarfs and one subdwarf. Because their data did not extend into the ultraviolet, however, they could not evaluate the differential correction to the  $U$  magnitude to obtain the correction to  $U - B$ , and it is the excess in  $U - B$  which acts as an index of line weakening and, therefore, to the corrections to  $B - V$  and to  $V$ .

Sandage and Eggen (1959) gave a procedure for correcting  $U - B$ ,  $B - V$ , and  $V$  by using the observed ultraviolet excess,  $\delta(U - B)$ , as such an index. These authors introduced the concept of a "blanketing line" in the  $U - B$ ,  $B - V$  diagram, along which a star would be shifted if its spectrum lines were weakened and ultimately removed altogether. They used the detailed measurements of the energy abstracted by the absorption lines in the solar spectrum by Wempe (1947) and by Michard (1950) to evaluate the changes  $\Delta U$ ,  $\Delta B$ , and  $\Delta V$  if all solar Fraunhofer lines were removed, and thereby obtained the slope,  $\Delta(U - B)/\Delta(B - V)$ , of the solar blanketing line. Because no data were available on the *change of slope* of the blanketing line on going along the main sequence in the  $U - B$ ,  $B - V$  diagram, Sandage and Eggen had to assume that the slope derived from the solar data applied at all points in the two-color diagram for  $0.4 < B - V < 0.8$ . Their elimination of the mild subdwarfs as a separate sequence in the  $M_{\text{bol}}$ ,  $\log T_e$  plane was thus based on the solar data alone.

The work reported in this paper was begun in 1956 to obtain blanketing lines for stars other than the sun in the relevant part of the  $U - B$ ,  $B - V$  diagram. Four stars were placed on the program—three normal dwarfs ( $\xi$  Peg, F7 V; 50 And, F8 V; 70 Vir, G5 V) and one well-known, extreme subdwarf (HD 19445, sdF). After the work was begun, Melbourne (1960) took up the problem, using a direct spectrum-scanner technique. The present paper gives the new blanketing data for our program stars and discusses these, together with Melbourne's material. Our final results are given in Table 4, where the corrections  $\Delta(B - V)$ ,  $\Delta(U - B)$ , and  $\Delta V$  are tabulated as a function of the observed  $B - V$  and the observed ultraviolet excess  $\delta(U - B)$ . These corrections are intended to reduce the observed radiation parameters to what would have been observed if  $\delta(U - B)$  were zero—viz., to reduce the data to Hyades-like stars. A preliminary report of part of this work was given at the Liège symposium in 1959 (Burbidge, Burbidge, Sandage, and Wildey 1959).

## II. THE SPECTRAL DATA

We require measurements of the ratio of the energy subtracted from the radiation field of a star by the Fraunhofer lines to the continuum energy at all relevant wavelengths.

High-dispersion spectra were obtained of  $\xi$  Peg, 50 And, 70 Vir, and HD 19445 with the coude spectrograph of the Mount Wilson 100-inch telescope. The spectra covered nearly the entire photometric range of the Johnson  $U, B, V$  filter system, i.e., from  $\lambda$  6300 to  $\lambda$  3300 Å. The dispersion we used was 10 Å/mm for wavelengths shortward of 5000 Å and 15 Å/mm for wavelengths longward of 5000 Å. The plates were Eastman Kodak baked IIa-O for the photographic region and baked IIa-D for the visual region. Calibration of the photographic plates was obtained in the usual manner with the Mount Wilson wedge-slit calibration spectrograph. The calibrations and the stellar spectra were made on plates taken from the same box, and the spectrograms were developed together in D19 for  $4\frac{1}{2}$  minutes. The spectrograms were then traced twice on Babcock's direct-intensity microphotometer. The first tracing was made with a magnification factor between plate and paper of 125. The second tracing had a magnification of 500. The former was used for drawing the continuum, which was then transferred to the 500 $\times$  tracings. The area contained within the absorption lines was then measured with a planimeter on the 500 $\times$  tracings, and the ratio between this area and the total area contained under the line representing the continuum was obtained for each 25 Å interval. Since the tracings record intensity directly, this ratio is the fractional energy,  $\epsilon(\lambda)$ , taken from the radiation field by the absorption lines.

The drawing of the continuum on the tracings is a most critical and difficult procedure. We made use of the Utrecht *Atlas* of the solar spectrum, with the corrections to the position of the continuum given by Michard (1950), and paying attention to the Chalonge "windows" in the spectrum (Canavaggia and Chalonge 1946). We were also guided by the size of the Balmer jump expected in these stars (Chalonge and Divan 1952; Divan 1956). This procedure made the placing of the continuum relatively unambiguous for  $\xi$  Peg (F7 V), 50 And (F8 V), and HD 19445 (sdF), but for 70 Vir (G5 V) it was not possible to do this with any certainty shortward of  $\lambda = 4800 \text{ \AA}$  because of the extreme

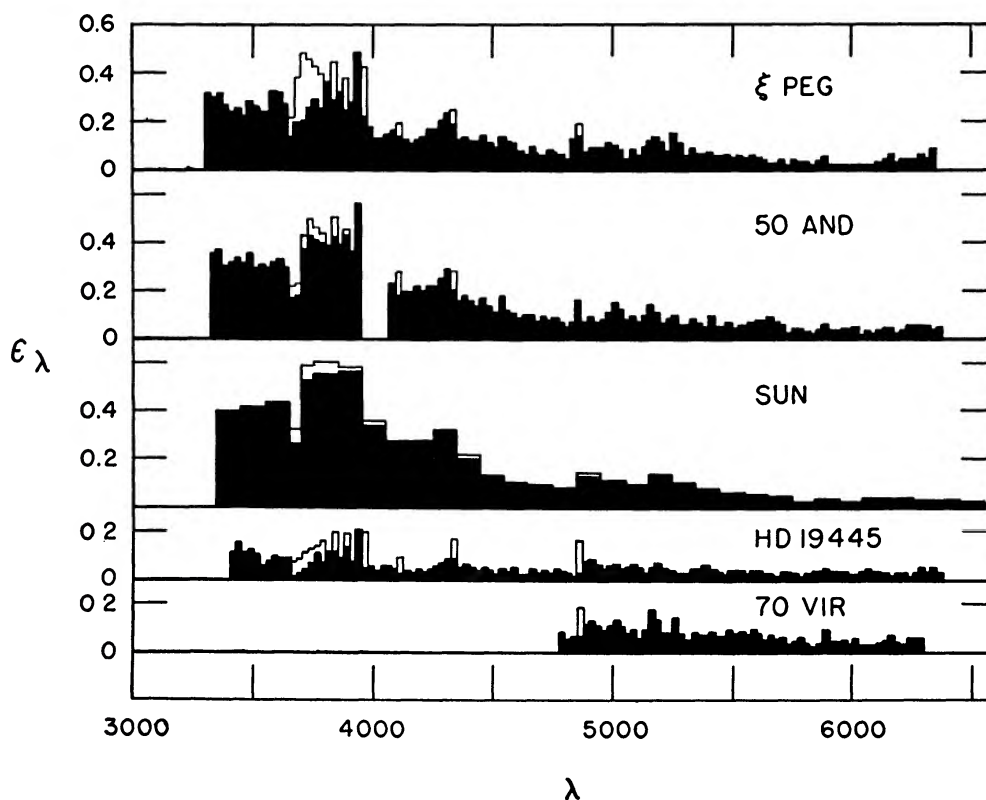


FIG. 1.—The fractional blocking coefficients,  $\epsilon(\lambda)$ , for the program stars. The data for the sun are from Michard (1950). The non-filled areas of the histograms represent absorption by the hydrogen lines.

crowding of the lines. We estimate that our systematic error in the continuum placement could be as large as 10 per cent in some regions of the spectrum. The error is smallest in the red and yellow spectral regions and increases toward the ultraviolet.

Since the purpose of this investigation is to make consistent the radiation parameters for stars in which the metals-to-hydrogen ratio is different but in which the hydrogen lines in the spectra are the same, it is somewhat artificial to include the hydrogen lines in the measurement of  $\epsilon(\lambda)$ , as is usually done, particularly as the continuous absorption shortward of the Balmer discontinuity, where the hydrogen lines crowd so closely that they merge, is of course retained. We have therefore measured  $\epsilon(\lambda)$  both with and without the hydrogen lines.

Table 1 gives the results for  $\epsilon(\lambda)$  (excluding the hydrogen lines) in 25 Å intervals. The data are shown graphically in Figure 1. The blocking of the hydrogen lines is shown explicitly by the non-filled-in areas in Figure 1. It should be noted that the data for 50 And are incomplete from  $\lambda 3950$  to  $\lambda 4075$ . The overlapping regions of the two high-

TABLE 1

MEASURED VALUES OF  $\xi(\lambda)$  (EXCLUDING HYDROGEN LINES)

$\lambda$	$\xi$ Peg	50 And	HD 19445	70 Vir
3300 - 3325	0.313	-	-	-
3325 - 3350	0.299	0.342	-	-
3350 - 3375	0.312	0.371	-	-
3375 - 3400	0.264	0.295	-	-
3400 - 3425	0.246	0.308	0.116	-
3425 - 3450	0.251	0.332	0.147	-
3450 - 3475	0.224	0.304	0.109	-
3475 - 3500	0.284	0.357	0.118	-
3500 - 3525	0.261	0.297	0.097	-
3525 - 3550	0.230	0.309	0.058	-
3550 - 3575	0.235	0.295	0.072	-
3575 - 3600	0.325	0.319	0.097	-
3600 - 3625	0.321	0.322	0.088	-
3625 - 3650	0.270	0.292	0.085	-
3650 - 3675	0.135	0.173	0.005	-
3675 - 3700	0.186	0.175	0.017	-
3700 - 3725	0.200	0.370	0.035	-
3725 - 3750	0.248	0.433	0.064	-
3750 - 3775	0.293	0.408	0.103	-
3775 - 3800	0.244	0.395	0.063	-
3800 - 3825	0.362	0.385	0.103	-
3825 - 3850	0.284	0.424	0.109	-
3850 - 3875	0.301	0.386	0.074	-
3875 - 3900	0.240	0.428	0.122	-
3900 - 3925	0.278	0.355	0.068	-
3925 - 3950	0.481	0.556	0.195	-
3950 - 3975	0.210	-	0.040	-
3975 - 4000	0.179	-	0.043	-
4000 - 4025	0.139	-	0.035	-
4025 - 4050	0.132	-	0.053	-

TABLE 1 (Cont.)

$\lambda$	$\xi$ Peg	50 And	HD 19445	70 Vir
4050 - 4075	0.143	-	0.051	-
4075 - 4100	0.155	0.230	0.041	-
4100 - 4125	0.138	0.210	0.020	-
4125 - 4150	0.104	0.199	0.035	-
4150 - 4175	0.106	0.192	0.025	-
4175 - 4200	0.117	0.213	0.033	-
4200 - 4225	0.125	0.194	0.028	-
4225 - 4250	0.167	0.213	0.039	-
4250 - 4275	0.161	0.219	0.051	-
4275 - 4300	0.191	0.248	0.066	-
4300 - 4325	0.231	0.285	0.080	-
4325 - 4350	0.180	0.224	0.080	-
4350 - 4375	0.114	0.155	0.045	-
4375 - 4400	0.124	0.168	0.053	-
4400 - 4425	0.114	0.155	0.043	-
4425 - 4450	0.110	0.135	0.034	-
4450 - 4475	0.131	0.164	0.042	-
4475 - 4500	0.101	0.130	0.030	-
4500 - 4525	0.080	0.105	0.019	-
4525 - 4550	0.132	0.170	0.039	-
4550 - 4575	0.104	0.117	0.036	-
4575 - 4600	0.101	0.105	0.041	-
4600 - 4625	0.067	0.086	0.019	-
4625 - 4650	0.059	0.096	0.018	-
4650 - 4675	0.086	0.099	0.028	-
4675 - 4700	0.059	0.077	0.022	-
4700 - 4725	0.047	0.098	0.032	-
4725 - 4750	0.066	0.073	0.024	-
4750 - 4775	0.059	0.086	0.030	-
4775 - 4800	0.058	0.061	0.023	0.075

TABLE 1 (Cont.)

$\lambda$	$\Sigma$ Peg	50 And	HD 19445	70 Vir
4800 - 4825	0.039	0.046	0.015	0.058
4825 - 4850	-	0.066	-	0.060
4850 - 4875	0.130	0.075	0.015	0.125
4875 - 4900	0.068	0.060	0.066	0.108
4900 - 4925	0.083	0.083	0.064	0.126
4925 - 4950	0.081	0.064	0.050	0.093
4950 - 4975	0.082	0.072	0.039	0.081
4975 - 5000	0.101	0.092	0.047	0.098
5000 - 5025	0.096	0.148	0.052	0.125
5025 - 5050	0.071	0.110	0.041	0.092
5050 - 5075	0.039	0.068	0.040	0.069
5075 - 5100	0.075	0.083	0.051	0.088
5100 - 5125	0.058	0.062	0.044	0.050
5125 - 5150	0.080	0.095	0.034	0.082
5150 - 5175	0.112	0.134	0.049	0.170
5175 - 5200	0.123	0.101	0.064	0.127
5200 - 5225	0.104	0.057	0.036	0.078
5225 - 5250	0.069	0.069	0.033	0.076
5250 - 5275	0.143	0.086	0.028	0.136
5275 - 5300	0.094	0.051	0.023	0.077
5300 - 5325	0.051	0.054	0.023	0.044
5325 - 5350	0.076	0.078	0.034	0.079
5350 - 5375	0.050	0.053	0.038	0.064
5375 - 5400	0.048	0.047	0.042	0.069
5400 - 5425	0.060	0.085	0.032	0.071
5425 - 5450	0.052	0.046	0.030	0.067
5450 - 5475	0.042	0.048	0.029	0.055
5475 - 5500	0.046	0.058	0.026	0.083
5500 - 5525	0.041	0.040	0.026	0.069
5525 - 5550	0.052	0.042	0.022	0.072

TABLE 1 (Cont.)

$\lambda$	$\Sigma$ Peg	50 And	HD 19445	70 Vir
5550 - 5575	0.049	0.048	0.020	0.066
5575 - 5600	0.051	0.063	0.029	0.085
5600 - 5625	0.049	0.065	0.026	0.071
5625 - 5650	0.038	0.076	0.017	0.041
5650 - 5675	0.030	0.082	0.018	0.063
5675 - 5700	0.024	0.062	0.015	0.050
5700 - 5725	0.027	0.057	0.022	0.052
5725 - 5750	0.011	0.026	0.021	0.029
5750 - 5775	0.031	0.034	0.022	0.039
5775 - 5800	0.025	0.038	0.015	0.055
5800 - 5825	0.020	0.023	0.019	0.022
5825 - 5850	0.012	0.012	0.022	0.009
5850 - 5875	0.028	0.027	0.021	0.026
5875 - 5900	0.043	0.055	0.030	0.089
5900 - 5925	0.020	0.025	0.025	0.038
5925 - 5950	0.018	0.024	0.022	0.031
5950 - 5975	0.014	0.028	0.021	0.035
5975 - 6000	0.014	0.031	0.014	0.028
6000 - 6025	0.018	0.040	0.018	0.044
6025 - 6050	0.012	0.017	0.025	0.028
6050 - 6075	0.017	0.028	0.031	0.022
6075 - 6100	0.129	0.020	0.030	0.025
6100 - 6125	0.026	0.029	0.024	0.033
6125 - 6150	0.033	0.038	0.016	0.041
6150 - 6175	0.053	0.038	0.010	0.063
6175 - 6200	0.021	0.014	0.012	0.037
6200 - 6225	0.027	0.022	0.013	0.027
6225 - 6250	0.028	0.046	0.015	0.051
6250 - 6275	0.022	0.046	0.020	0.048
6275 - 6300	0.044	0.045	0.041	0.047
6300 - 6325	0.042	0.046	0.026	-
6325 - 6350	0.080	0.039	0.042	-

dispersion spectrograms were not dense enough in this region to obtain reliable measurements. In the computations that follow, values of  $\epsilon(\lambda)$  for this region were obtained by assuming that the ratio of  $\epsilon(\lambda)$  for 50 And to  $\epsilon(\lambda)$  for  $\xi$  Peg was the same on either side of the break.

### III. ANALYSIS

As was pointed out previously (Sandage and Eggen 1959; Burbidge *et al.* 1960), the Fraunhofer lines affect the observed energy distribution of a star in at least three ways.

1. The lines block the radiation of the continuum. The observed emergent flux at any wavelength would thereby be reduced if this effect were operating alone. The fractional energy subtracted from the radiation beam is  $\epsilon(\lambda)$ . Then the heterochromatic magnitude difference due to this blocking is

$$\Delta \text{ mag.} = 2.5 \log \left\{ \frac{\int_{\lambda_1}^{\lambda_2} F(\lambda) S(\lambda) d\lambda}{\int_{\lambda_1}^{\lambda_2} F(\lambda) S(\lambda) [1 - \epsilon(\lambda)] d\lambda} \right\}, \quad (1)$$

where  $F(\lambda)$  is the continuum flux,  $S(\lambda)$  is the sensitivity function of the photometric system (telescope, filters, photocell), and  $\lambda_1$  and  $\lambda_2$  are the cutoff wavelengths of the band pass being considered.

2. The blocked radiation must ultimately escape from the star in regions between the lines, i.e., no net energy can be lost to the radiation field because of the presence of absorption lines. The escape is accomplished by a raising of the level of the continuum over the level it would have had in the absence of lines. This is brought about by an increased temperature in the relevant photospheric layers caused by the radiation back-scattered by the lines. The size of this back-warming effect can be estimated as follows. Consider two stars of the same luminosity,  $L$ , and radius,  $R$ , and therefore of the same effective temperature. Let star 1 have normal strengths of the Fraunhofer lines, while star 2 is without lines. Each radiates the same bolometric energy,  $L$ . The energy subtracted from star 1 by all the lines is given by

$$\text{Energy subtracted} = \int_0^{\infty} \epsilon(\lambda) F_1(\lambda) d\lambda. \quad (2)$$

Define  $\eta$  as the integrated blocking coefficient by

$$\eta \equiv \frac{\int_0^{\infty} \epsilon(\lambda) F_1(\lambda) d\lambda}{\int_0^{\infty} F_1(\lambda) d\lambda}. \quad (3)$$

Equation (2) then becomes

$$\text{Energy subtracted} = \eta \int_0^{\infty} F_1(\lambda) d\lambda, \quad (4)$$

and, because this energy cannot be stored, it must escape between the absorption lines of star 1. If we consider continuum levels only, it follows from  $L_1 = L_2$  that

$$\int_0^{\infty} F_2(\lambda) d\lambda = (1 - \eta) \int_0^{\infty} F_1(\lambda) d\lambda. \quad (5)$$

The continuum levels  $F_1$  and  $F_2$  can be computed from model atmospheres, characterized by effective temperatures  $(T_e)_1$  and  $(T_e)_2$ , and defined by

$$\sigma (T_e)_i^4 = \pi \int_0^{\infty} F_i(\lambda) d\lambda.$$

Consequently, the model-atmosphere tables must be entered at different effective (continuum) temperatures to obtain  $F_1(\lambda)$  and  $F_2(\lambda)$ . Equation (5) shows that

$$(T_e)_2^4 = (1 - \eta)(T_e)_1^4. \quad (6)$$

We may summarize as follows: if all the lines were removed from a star, the level of its continuum would drop from its value  $F_1(\lambda)$  to a lower value  $F_2(\lambda)$ . The change in the  $U$ ,  $B$ , and  $V$  magnitudes due to this back-warming effect alone is

$$\Delta \text{ mag.} = 2.5 \log \frac{\int_{\lambda_1}^{\lambda_2} F_1(\lambda) S(\lambda) d\lambda}{\int_{\lambda_1}^{\lambda_2} F_2(\lambda) S(\lambda) d\lambda}. \quad (7)$$

3. A change in the metal abundance could change the atmospheric opacity and therefore the wavelength distribution of the emergent flux. This third effect has been shown to be negligible for stars in the relevant temperature range (Swihart and Fischel 1961).

The total effect on the  $U$ ,  $B$ , and  $V$  magnitudes caused by removing the Fraunhofer lines from a star is the sum of equations (1) and (7). The blocking effect described by equation (1) gives *brighter* magnitudes at all wavelengths as the lines are *removed*. The back-warming effect of equation (7) gives *fainter* magnitudes at all wavelengths as the lines are removed. The two effects are therefore to be added with opposite sign. As will be seen in Section IV, the blocking is usually larger than the back-warming effect in the  $U$  and  $B$  band pass for the four stars on our program. The  $U$  and  $B$  magnitudes therefore become brighter as the lines are removed. However, back-warming is greater than blocking for all band passes redward of that given by the  $B$  filter, so the stars become *fainter* in  $V$  by line *removal*.

#### IV. RESULTS

The data given in Table 1 were analyzed by the method discussed in Section III. The blocking coefficient  $\eta$  was obtained for the four program stars over the spectral region studied, i.e., from  $\lambda$  3300 to  $\lambda$  6300 Å. The values derived over this range were 0.140 for  $\xi$  Peg, 0.160 for 50 And, 0.190 for the sun, and 0.054 for HD 19445. Over the entire spectrum Michard derived the integrated blanketing coefficient to be 0.124 for the sun. Assuming  $\eta$  over the entire spectrum to be in the same proportion as the values in our measured range, we derive the values of  $\eta$  over the entire spectrum given in the top row of Table 2.

The true effective temperatures  $(T_e)_2$  are given in Table 2, together with the temperature  $(T_e)_1$  of the photospheric model, which has the same continuum level between the lines as the real star. The adopted true effective temperature of HD 19445 was 5760° K, corresponding to a star very slightly earlier in spectral type than G2 V. In the course of the work, by comparing the spectra of the program stars, we found that the excitation temperature of HD 19445 given by the Fe I lines agrees much better with the excitation temperature of the sun than it does with that of an F7 V star, which was the type assigned by Miss Roman.

Equations (1) and (7) were then used to compute the effect of blocking and of back-warming on  $U$ ,  $B$ , and  $V$ . The sensitivity functions  $S(\lambda)$  were taken from Johnson's definition of the  $U$ ,  $B$ ,  $V$  system (1955) as modified by Code (Melbourne 1960) for atmospheric cutoff. The flux values  $F(\lambda)$  were taken from the atmospheric models of de Jager and Neven (1957), by interpolating for the appropriate values of  $T_0 = (2)^{-1/4} T_e$  and surface gravity. The interpolation equation used to obtain the flux is

$$\frac{\log F(T_3) - \log F(T_1)}{\log F(T_2) - \log F(T_1)} = \frac{T_2}{T_3} \left( \frac{T_3 - T_1}{T_2 - T_1} \right), \quad (8)$$

where values for  $T_1$  and  $T_2$  are tabulated and values for  $T_3$  are to be determined. This equation assumes black-body behavior between the entries.

The results of the calculations are given in Table 2, where the change in  $U, B,$  and  $V$  due to blocking (with and without the hydrogen lines removed), the change due to back-warming, and the combined effect of both blocking and back-warming are tabulated. For example, if all lines but those due to hydrogen were removed from the solar spectrum, the  $U$  magnitude at the center of the solar disk would become brighter by  $0^m616$  by the blocking effect alone but would become fainter by  $0^m220$  because of removal of the back-warming effect of the lines. The total effect would be that the  $U$  magnitude would be  $0^m396$  brighter. Similar results apply to the  $B$  and  $V$  magnitudes, with the end result

TABLE 2  
BLANKETING DATA FOR PROGRAM STARS

		$\xi$ Peg	50 And	Sun (Center)	HD 19445
$\eta$		0 091	0 104	0 124	0 035
$(T_e)_1$ ° K . .		6421	6321	6201	5812
$(T_e)_2$ ° K .		6270	6150	6000	5760
$\Delta T(\eta)$ ° K		151	171	201	52
Blocking (remove all lines)	$\Delta U$	-0 <sup>m</sup> 423	-0 <sup>m</sup> 468	-0 <sup>m</sup> 646	-0 <sup>m</sup> 123
	$\Delta B$ . .	- 169	- 221	- 274	- 061
	$\Delta V$ . .	- 064	- 067	- 074	- 033
Blocking (remove all but H lines)	$\Delta U$	- 315	- 437	- 616	- 093
	$\Delta B$	- 154	- 214	- 262	- 049
	$\Delta V$	- 064	- 067	- 074	- 033
Back-warming	$\Delta U$	+ 150	+ 167	+ 220	+ 064
	$\Delta B$	+ 134	+ 167	+ 204	+ 059
	$\Delta V$ .	+ 109	+ 133	+ 173	+ 058
Combined blanketing effect (leaving H lines in)	$\Delta U$	- 165	- 270	- 396	- 029
	$\Delta B$ . . .	- 020	- 047	- 058	+ 010
	$\Delta V$	+ 045	+ 066	+ 099	+ 025
	$\Delta(B-V)$	- 065	- 113	- 157	- 015
	$\Delta(U-B)$	-0 145	-0 223	-0 338	-0 039

that removing all lines but hydrogen would cause the sun to become bluer by  $\Delta(B - V) = 0^m157$  and  $\Delta(U - B) = 0^m338$ . These numbers determine the slope of the blanketing vector of the sun in the  $U - B, B - V$  diagram.

Tables 3A and 3B summarize all the data of this kind now available. The first six entries of Table 3A are from Melbourne's study, while the next three are from the present work. Columns 1 and 2 give the observed values of  $B - V$  and  $U - B$ ; columns 3, 4, and 5 give the total (blocking + back-warming) values of  $\Delta(B - V), \Delta(U - B),$  and  $\Delta V$  obtained by removing all but the hydrogen lines from the spectrum of the star in question. Columns 6 and 7 show the continuum colors,  $(B - V)_{MR}$  and  $(U - B)_{MR}$ , obtained by applying columns 3 and 4 to 1 and 2. Column 8 gives the slope of the blanketing line,  $\Delta(U - B)/\Delta(B - V)$ ; column 9 gives the ratio of  $\Delta V$  to  $\Delta(B - V)$ . Finally, column 10 gives the  $B - V$  that the star would have on the Hyades  $U - B, B - V$  diagram; this is obtained by moving the star from its observed  $B - V$  value back along its blanketing line to the intersection with the mean Hyades  $U - B, B - V$  relation.

Table 3B gives the data for the two subdwarfs HD 19445 and HD 140283, the latter being taken from Melbourne's work. These stars are so nearly line-free that the residual effect on  $B - V$  and  $U - B$  caused by removing the lines is small. Our values for

HD 19445 in Table 2 are  $\Delta(B - V) = -0^m015$  and  $\Delta(U - B) = -0^m039$ . Consequently, the slope of the blanketing vector is poorly determined from these data, for its extent backward away from the Hyades line to the position of a line-free star is so short. If the blanketing vector could be extended the relatively long distance downward toward the Hyades line, this would provide a more powerful method for determining the slope. Accordingly, we have adopted Melbourne's (1960) values of  $T_e$  for these two stars, have gone to the adopted relation  $(B - V)_{\text{Hyades}} = f(T_e)$ , and have found the differences  $\Delta(B - V)$  and  $\Delta(U - B)$  between the observed values (cols. 1 and 2) and the Hyades

TABLE 3A  
DATA FOR MELBOURNE'S STARS PLUS PRESENT PROGRAM STARS

Star	$(B - V)_0$ (1)	$(U - B)_0$ (2)	$\Delta(B - V)$ (3)	$\Delta(U - B)$ (4)	$\Delta V$ (5)	$(B - V)_{MR}$ (6)	$(U - B)_{MR}$ (7)	$\Delta(U - B)/\Delta(B - V)$ (8)	$\Delta V/\Delta(B - V)$ (9)	$(B - V)_{m.s.}$ (10)
$\sigma$ Boo	0 37	-0 09	-0 07	-0 13	-0 07	0 30	-0 22	1 86	1 000	0 420
$\pi^3$ Ori	46	00	- 12	- 21	- 05	34	- 21	1 75	0 416	.465
110 Her.	46	00	- 13	- 23	- 09	33	- 23	1.77	0 69	465
$\beta$ Com	56	+ 05	- 16	- 33	- 06	40	- 28	2 06	0 38	60
Sun	.	.	- 17	-.36	- 09	.	.	2 12	0 53	645
51 Peg	68	+ 20	- 20	- 49	- 08	48	- 29	2 45	0 40	70
$\xi$ Peg	50	- 03	- 065	- 145	- 045	435	- 175	2 23	0 69	545
50 And	54	+ 06	- 113	- 223	- 066	427	- 163	1 97	0 58	550
Sun .	0 60	+0 09	-0 157	-0 338	-0 099	0 443	-0 248	2 15	0 63	0 645

TABLE 3B  
DATA FOR TWO SUBDWARF STARS

Star	$(B - V)_0$ (1)	$(U - B)_0$ (2)	$(B - V)_{m.s.}$ (3)	$(U - B)_{m.s.}$ (4)	$\Delta(B - V)$ (5)	$\Delta(U - B)$ (6)	$\Delta(U - B)/\Delta(B - V)$ (7)
HD 19445.	0 46	-0 24	0 61	0 14	-0 15	-0 38	2 54
HD 140283	0 51	-0 23	0 70	0 25	-0 19	-0 48	2 52

main-sequence values (cols. 3 and 4). These are tabulated in columns 5 and 6 of Table 3B, and their ratio yields the slope of the blanketing vector given in column 7.

Figure 2 shows the blanketing lines for the ten stars in Tables 3A and 3B. Filled circles represent observed values; crosses represent the line-free positions. It is evident that a progressive change in slope of the blanketing line is present. This is shown more clearly in Figure 3, where the slope  $\Delta(U - B)/\Delta(B - V)$  is plotted against the Hyades-main-sequence  $B - V$  colors. Melbourne's five stars of Table 3A are filled circles, our three stars are crosses, and the two subdwarfs are triangles. The agreement is excellent and shows that the various methods used to obtain the data are quite consistent. Finally, Figure 4 shows the variation of  $\Delta V/\Delta(B - V)$  with  $B - V$  on the main sequence.

#### V. THE CORRECTION PROCEDURE

The notation used in this section is illustrated in Figure 5. Suppose a weak-lined star is observed to have colors  $(U - B)_{\text{obs}}$  and  $(B - V)_{\text{obs}}$ . Relative to the Hyades line, the star has an ultraviolet excess  $\delta(U - B)$ , defined as in Figure 5. Figure 3 is entered with  $(B - V)_{\text{obs}}$ , and a blanketing line with the slope thereby obtained is drawn through the

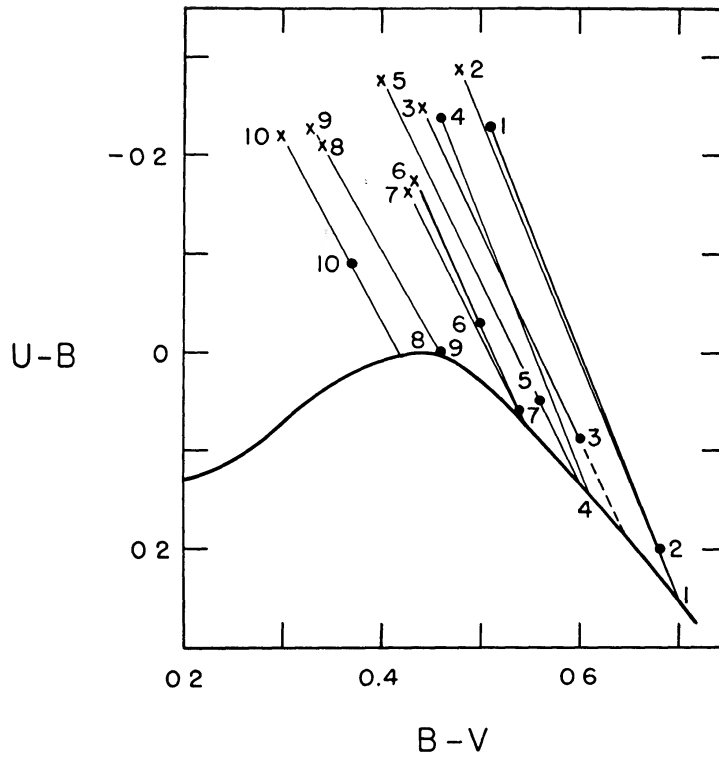


FIG. 2.—The blanketing vectors for the stars in Table 3. The filled circles represent observed points. The crosses are the line-free colors. The identifications are: (1) HD 140283; (2) 51 Peg; (3) sun; (4) HD 19445; (5)  $\beta$  Com; (6)  $\xi$  Peg; (7) 50 And; (8)  $\pi^3$  Ori; (9) 110 Her; (10)  $\sigma$  Boo. Data for stars 1, 2, 5, 8, 9, and 10 are from Melbourne (1960).

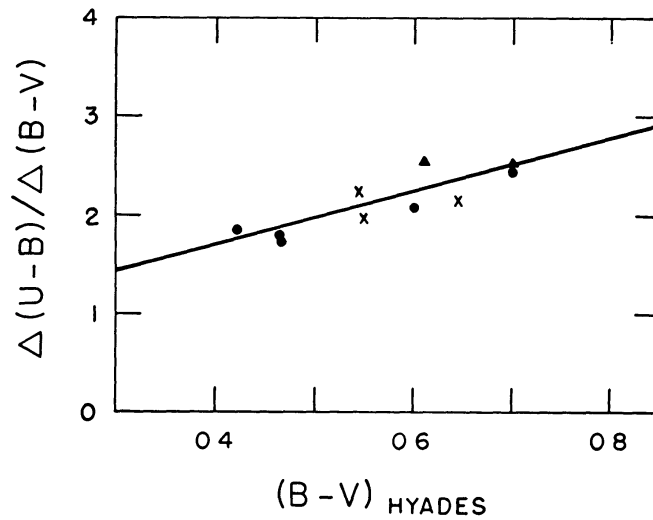


FIG. 3.—The slope of the blanketing lines as a function of their  $B - V$  intersection with the Hyades line. The dots are Melbourne's data; the crosses represent our data for  $\xi$  Peg, 50 And, and the sun; and the triangles are the subdwarfs HD 19445 and HD 140283.

observed point. This line intersects the Hyades line as shown,  $(B - V)_{\text{Hyades}}$  is obtained, and Figure 3 is again entered with this value for an improved value of the slope of the blanketing line. The vectors  $\Delta(U - B)$  and  $\Delta(B - V)$  obtained by iteration in this way are the corrections that must be applied to the observed colors to correct for the differential line blanketing between the star in question and Hyades-like stars. The data of Figure 4 then give the  $\Delta V$  correction, once  $\Delta(B - V)$  is known.

It is clear that the corrections  $\Delta(B - V)$ ,  $\Delta(U - B)$ , and  $\Delta V$  are unique functions determined when  $\delta(U - B)$  and  $(B - V)_{\text{obs}}$  are known. A correction table has been prepared in this way and is given in Table 4. In the calculations, the slopes of the blanketing

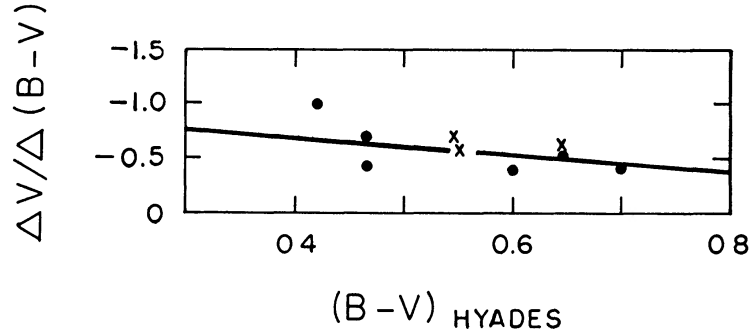


FIG. 4.—The relation between  $\Delta V$ ,  $\Delta(B - V)$ , and the  $B - V$  intersection of the blanketing lines with the Hyades line.

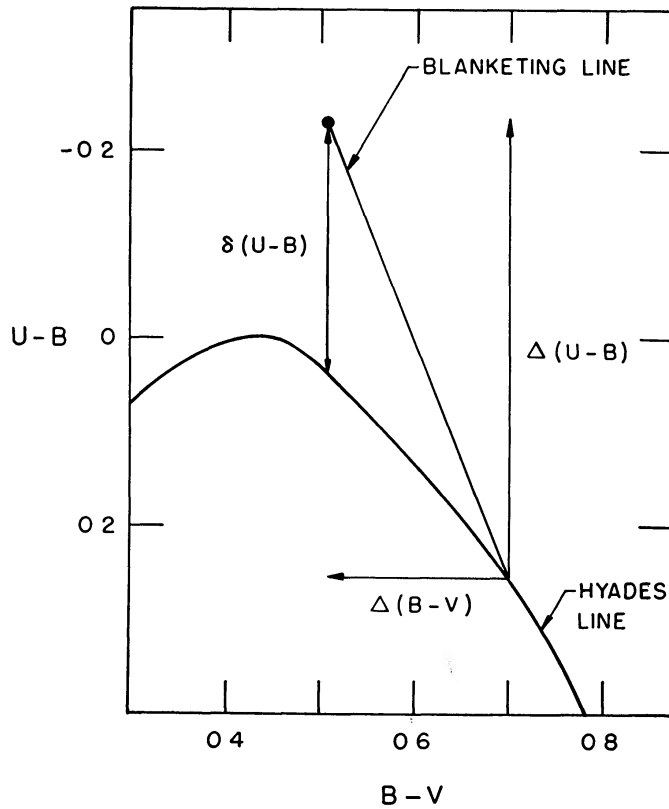


FIG. 5.—The definitions of  $\Delta(B - V)$ ,  $\Delta(U - B)$ , and the ultraviolet excess,  $\delta(U - B)$

Table 4  
 Corrections to UVB Photometry for Varying Ultraviolet Excess \*

$\delta(U-B)$	0.00	0.02	0.04	0.06	0.08	0.10	0.12	0.14	0.16	0.18	0.20	0.22	0.24	0.26	0.28	0.30	0.32	0.34	0.36	0.38	0.40
0.30	0.000	0.010	0.017	0.026	0.035	0.044	0.052	0.060	0.070	0.079	0.088	0.096	.105	0.114	0.123	0.131	.140	.148	.159	.170	
	0.000	0.014	0.025	0.039	0.054	0.068	0.082	0.096	0.113	0.130	0.146	0.162	0.179	0.198	0.216	0.232	0.252	0.271	0.296	.321	
	0.000	0.007	0.013	0.019	0.025	0.032	0.037	0.042	0.049	0.055	0.060	0.064	0.069	0.075	0.080	0.085	0.091	0.095	0.102	0.105	
0.35	0.000	0.010	0.018	0.028	0.037	0.048	0.057	0.066	0.075	0.085	0.094	0.105	0.116	0.130	0.142	0.154	0.162	0.180	0.194	-	
	0.000	0.016	0.029	0.046	0.062	0.081	0.098	0.115	0.133	0.152	0.171	0.194	0.218	0.248	0.276	0.304	0.324	0.369	0.404	-	
	0.000	0.007	0.013	0.019	0.025	0.032	0.038	0.043	0.049	0.055	0.060	0.067	0.073	0.079	0.086	0.093	0.096	0.103	0.109	-	
0.40	0.000	0.010	0.020	0.030	0.040	0.051	0.063	0.075	0.090	0.105	0.118	0.133	0.148	0.161	0.173	0.185	0.197	-	-	-	
	0.000	0.017	0.035	0.053	0.072	0.094	0.117	0.143	0.175	0.208	0.237	0.274	0.310	0.343	0.374	0.406	0.440	-	-	-	
	0.000	0.007	0.013	0.019	0.026	0.033	0.040	0.046	0.055	0.063	0.070	0.076	0.083	0.089	0.093	0.100	0.107	-	-	-	
0.45	0.000	0.016	0.030	0.045	0.060	0.075	0.092	0.107	0.120	0.135	0.150	0.162	0.175	0.187	0.200	0.210	0.221	0.231	0.241	-	
	0.000	0.030	0.057	0.088	0.120	0.152	0.191	0.227	0.258	0.297	0.336	0.368	0.402	0.438	0.475	0.504	0.538	0.566	0.598	-	
	0.000	0.010	0.018	0.027	0.036	0.044	0.051	0.059	0.066	0.073	0.078	0.083	0.089	0.093	0.098	0.101	0.103	0.106	0.109	-	
0.50	0.000	0.020	0.039	0.053	0.067	0.083	0.100	0.114	0.127	0.141	0.154	0.165	0.179	0.188	0.200	0.211	0.225	0.240	0.255	0.270	0.282
	0.000	0.040	0.081	0.112	0.143	0.182	0.224	0.259	0.294	0.332	0.368	0.398	0.439	0.466	0.500	0.536	0.579	0.630	0.678	0.729	0.770
	0.000	0.012	0.022	0.030	0.037	0.045	0.052	0.058	0.064	0.070	0.075	0.078	0.082	0.087	0.091	0.095	0.099	0.103	0.105	0.108	0.111
0.55	0.000	0.018	0.034	0.050	0.065	0.080	0.092	0.106	0.121	0.134	0.147	0.162	0.177	0.194	0.210	0.225	0.238	0.250	-	-	
	0.000	0.039	0.075	0.112	0.148	0.185	0.216	0.254	0.294	0.330	0.368	0.411	0.458	0.510	0.561	0.614	0.655	0.695	-	-	
	0.000	0.010	0.018	0.026	0.033	0.040	0.046	0.051	0.056	0.062	0.066	0.073	0.078	0.082	0.086	0.090	0.091	0.092	-	-	
0.60	0.000	0.017	0.032	0.047	0.062	0.076	0.090	0.106	0.122	0.140	0.157	0.175	0.192	0.205	0.214	0.221	0.225	-	-	-	
	0.000	0.039	0.074	0.112	0.149	0.186	0.224	0.267	0.312	0.367	0.417	0.475	0.530	0.572	0.604	0.628	0.644	-	-	-	
	0.000	0.009	0.016	0.023	0.030	0.035	0.041	0.048	0.054	0.059	0.064	0.070	0.073	0.076	0.077	0.080	0.079	-	-	-	
0.65	0.000	0.018	0.031	0.046	0.063	0.080	0.101	0.122	0.139	0.152	0.163	0.172	-	-	-	-	-	-	-	-	
	0.000	0.044	0.076	0.115	0.160	0.207	0.268	0.329	0.382	0.423	0.456	0.489	-	-	-	-	-	-	-	-	
	0.000	0.009	0.014	0.021	0.028	0.034	0.042	0.049	0.054	0.056	0.059	0.060	-	-	-	-	-	-	-	-	
0.70	0.000	0.020	0.040	0.060	0.084	0.100	0.113	0.123	-	-	-	-	-	-	-	-	-	-	-	-	
	0.000	0.051	0.105	0.160	0.230	0.278	0.318	0.350	-	-	-	-	-	-	-	-	-	-	-	-	
	0.000	0.009	0.011	0.024	0.033	0.037	0.041	0.043	-	-	-	-	-	-	-	-	-	-	-	-	
0.75	0.000	0.025	0.045	0.060	0.070	0.080	-	-	-	-	-	-	-	-	-	-	-	-	-	-	
	0.000	0.068	0.124	0.168	0.199	0.230	-	-	-	-	-	-	-	-	-	-	-	-	-	-	
	0.000	0.010	0.017	0.022	0.025	0.028	-	-	-	-	-	-	-	-	-	-	-	-	-	-	
0.80	0.000	0.025	0.050	-	-	-	-	-	-	-	-	-	-	-	-	-	-	-	-	-	
	0.000	0.071	0.146	-	-	-	-	-	-	-	-	-	-	-	-	-	-	-	-	-	
	0.000	0.008	0.017	-	-	-	-	-	-	-	-	-	-	-	-	-	-	-	-	-	

\*The tabulated quantities are:  $\begin{cases} +\Delta(B-V) \\ +\Delta(U-B) \\ -\Delta V \end{cases}$

lines were adopted from Figure 3 as

$$\frac{\Delta(U - B)}{\Delta(B - V)} = 2.70(B - V)_{\text{Hyades}} + 0.62. \quad (9)$$

The  $V$  function was adopted from Figure 4 as

$$\frac{\Delta V}{\Delta(B - V)} = 0.75(B - V)_{\text{Hyades}} - 0.97. \quad (10)$$

The following example illustrates the use of Table 4. Suppose a star is observed to have  $V = 8.00$ ,  $B - V = 0.50$ ,  $U - B = -0.13$ . Reference to the two-color diagram shows that Hyades-like stars at  $B - V = 0.50$  should have  $U - B = 0.03$ . Therefore,  $\delta(U - B) = 0.16$ . Table 4 shows that  $\Delta(B - V) = 0.127$ ,  $\Delta(U - B) = 0.294$ , and  $\Delta V = -0.064$  for  $(B - V)_{\text{obs}} = 0.50$ ,  $\delta(U - B) = 0.16$ . Therefore, if the Fraunhofer lines were as strong as those in the Hyades stars, the star would have been observed to have  $B - V = 0.63$ ,  $U - B = 0.16$ , and  $V = 7.94$ .

It is of interest to compare Table 4 with the single-entry table of Sandage and Eggen (1959, Table IV), based only on the solar blanketing line. The slope of the solar line adopted by these authors was  $\Delta(U - B)/\Delta(B - V) = 0.40/0.21 = 1.91$ . This is in fair agreement with Figure 3 at  $(B - V)_{\text{Hyades}} = 0.645$ . Therefore, the conclusions reached in the earlier study concerning the absence of a separate subdwarf sequence in the  $M_{\text{bol}}$ ,  $\log T_e$  plane for mild subdwarfs should not be changed by the present paper.

#### REFERENCES

- Burbidge, E. M., Burbidge, G. R., Sandage, A. R., and Wildey, R. L. 1959, *Colloque International d'Astrophysique, Liège*, No. 9, p. 427.  
 Canavaggia, R., and Chalonge, D. 1946, *Ann. d'ap.*, 9, 143.  
 Chalonge, D., and Divan, L. 1952, *Ann. d'ap.*, 15, 201.  
 Code, A. D. 1959, *Ap. J.*, 130, 473.  
 Divan, L. 1956, *Ann. d'ap.*, 19, 287.  
 Jager, C. de, and Nevén, L. 1957, *Ann. Obs. R. Belgique*, Vol. 8, Part 1.  
 Johnson, H. L. 1955, *Ann. d'ap.*, 18, 292.  
 Melbourne, W. G. 1960, *Ap. J.*, 132, 101.  
 Michard, R. 1950, *B.A.N.*, 11, 227.  
 Roman, N. G. 1954, *A.J.*, 59, 307.  
 Sandage, A. R., and Eggen, O. J. 1959, *M.N.*, 119, 278.  
 Schwarzschild, M., Searle, L., and Howard, R. 1955, *Ap. J.*, 122, 353.  
 Swihart, T. L., and Fischel, D. 1961, *Ap. J. Suppl.*, 5, 291.  
 Wempe, J. 1947, *A.N.*, 275, 97.